Current Chemistry Letters 8 (2019) 39–52

Contents lists available at GrowingScience

Current Chemistry Letters

homepage: www.GrowingScience.com

Synthesis, spectroscopic characterization, crystal structure and Hirshfeld surface analysis of Co(III), Ni(II) and VO(IV) metal complexes with a novel Schiff base ligand and their antimicrobial activities

Disha Sharma[a] and Hosakere D. Revanasiddappa[a*]

[a]*Department of Chemistry, University of Mysore, Manasagangothri, Mysuru 570 006, Karnataka, India*

C H R O N I C L E

Article history:
Received September 3, 2018
Received in revised form
November 18, 2018
Accepted December 18, 2018
Available online
December 19, 2018

Keywords:
Schiff base
Metal complexes
X-ray crystal structure
Hirshfeld surface analysis
Antibacterial and antifungal

A B S T R A C T

A new series of transition metal complexes of Co(III), Ni(II) and VO(IV) was synthesized with the bidentate Schiff base ligand (HL) derived from the condensation of 2-amino-3-benzyloxypyridine and 5-bromo salicylaldehyde. The synthesized Schiff base ligand and its metal complexes C1-C6 were structurally characterized by satisfactory elemental analysis, spectral studies such as (Mass, IR, ^{1}H and ^{13}C NMR, conductance measurement, UV-vis and magnetic measurements) and thermal studies. The structure of HL was authenticated by X-ray single-crystal analysis. Hirshfeld surface analysis was carried out to understand the nature of intermolecular contacts, the fingerprint plot provides the information about the percentage contribution. Square-pyramidal geometry is proposed for VO(IV) complexes whereas octahedral geometry for Co(III) and Ni(II) complexes. The Schiff base ligand and its metal complexes have been tested *in vitro* for their antibacterial activities by using well diffusion method against Gram positive bacteria *B. subtilis*, *S. aureus* and Gram negative bacteria *S. typhi*, *E. coli* and antifungal activities against *A. niger*, *A. flavus*, *C. albicans* and *A. Solani*. The antimicrobial activity data show that metal complexes are more potent than the parent ligand.

1. Introduction

Schiff bases derived from an amino and carbonyl compound are an important class of ligands that coordinate to metal ions via azomethine nitrogen and have been studied extensively. In azomethine derivatives, the C=N linkage is essential for biological activity, several azomethine have been reported to possess remarkable antimicrobial,[1] anticancer[2] and antimalarial activities.[3,4]

For the past two decades, Schiff bases were in constant emergence because of their simplicity in preparation and diversity in reactions.[5] In comparison to 4d or 5d metal complexes, complexes of 3d transition metal ion exhibit beneficial properties as low toxicity and easily penetrate to the cell membrane of microbes.[6] Literature survey shows that Schiff bases show bacteriostatic and bactericidal activity.[7] Schiff bases containing *o*-vanillin possesses antifungal, antibacterial properties[8] and it acts as a weak inhibitor of tyrosinase, display both antimutagenic and co-mutagenic properties in *E.coli.*[9] Imines are possess antibacterial and more antifungal activities. The compounds having antimicrobial activity may act either by killing the microbe or by inhibiting multiplication of the microbe by blocking

* Corresponding author. Tel: +919449271137, +91821-2419669
E-mail address: hdrevanasiddappa@yahoo.com (H. D. Revanasiddappa)

doi: 10.5267/j.ccl.2018.012.003

their active sites.[10] Schiff bases derived from salicylaldehydes are well known as polydentate ligands, coordinating as deprotonated or neutral forms.[11] Thus, the chemical literature prompted us to prepare the transition metal complexes with new Schiff base ligand, here we present the synthesis and characterization of new Schiff base ligand derived from 2-amino-3-benzyloxypyridine and 5-bromo salicylaldehyde as well as its Co(III), Ni(II) and VO(IV) metal complexes. Further, the structures of the complexes are elucidated by various spectral techniques. The bio-relevancy of these complexes have been professionally studied and explored by antimicrobial studies. The crystal structure of the HL ligand was studied by X-ray analysis and to same is reported.

2. Results and discussion

The obtained complexes are coloured powders, stable in air, insoluble in water and other common solvents but are easily soluble in polar coordinating solvents such as DMF and DMSO. Elemental analysis of the complexes indicates the stoichiometry to be 1:2 metal: ligand for C1, C3 and C5 and 1:1:1 metal: ligand: 1, 10-phenanthroline for C2, C4 and C6. The analytical data of the ligand and metal complexes are given in **Table 1** and are in good agreement with the proposed formulation. The molar conductivity values corresponding to the Co(III), Ni(II) and VO(IV) complexes at 10^{-3} M in DMSO in the range of 9.37-17.55 $\Omega^{-1}cm^2\,mol^{-1}$ and in this way a structural formula of non-electrolyte for these complexes can be assigned.

Table. 1. Elemental analysis and physical data of Schiff base ligand and its metal complexes.

Compound	Molecular Formula	Yield (%)	Calculated (Found) (%)			Magnetic moment μ_{eff} BM
			(%)C	(%)H	(%)N	
HL	$C_{19}H_{15}BrN_2O_2$	87	59.55 (60.07)	3.95 (3.14)	7.31 (6.96)	—
C1	$CoC_{38}H_{30}Br_2ClN_4O_5$	75	52.97 (53.05)	4.00 (4.32)	6.18 (6.37)	—
C2	$CoC_{31}H_{22}BrCl_2N_4O_2$	69	53.78 (53.86)	3.20 (3.49)	8.09 (8.47)	—
C3	$NiC_{38}H_{32}Br_2N_4O_6$	76	54.03 (54.29)	4.31 (4.75)	6.30 (6.53)	3.3
C4	Ni $C_{31}H_{26}BrN_4O_4$	81	55.66 (55.87)	3.99 (4.09)	8.53 (8.71)	3.4
C5	$VC_{38}H_{28}Br_2N_4O_5$	63	55.77 (55.94)	3.98 (4.17)	6.50 (6.71)	1.71
C6	$VC_{31}H_{22}BrN_4O_3$	71	59.16 (55.37)	3.52 (3.84)	8.90 (9.05)	1.74

2.1. Description of the X-ray structure of HL

Single crystal X-ray diffraction analysis confirms the molecular structure of the title ligand HL. ORTEP view structure of the title ligand is shown in **Fig. 1.** The optimized parameters (bond lengths and bond angles) are in good agreement with the standard values, the list of selected bond lengths and bond angles are given in **Tables 2** and **Table 3**. The title ligand exists in orthorhombic crystal system with $Pca2_1$ space group. The unit cell parameters are a = 14.240(3) Å, b = 16.090(3) Å, c = 7.2170(13) Å and V= 1653.5(5) $Å^3$. The average length of the N1=C7 bond is 1.289(15) Å, and bond angle of N1-C7-C6 is 120.0(9)° obtained. In the crystal, two types of intermolecular hydrogen-bonding interactions are present **(Table 4)**. The primary strong O2-H2---N1 hydrogen bond between the imine group and a carbonyl group generates butterfly structure along the b-axis direction and the secondary

weak methyl C19-H19---O1^{i} and C19-H19---O2^{i} (where, i=-x+1,-y+1,-z+1/2) hydrogen-bonding interactions as depicted in **Fig. 2**.

Table. 2. Selected bond distances (Å) for HL.

Atom	Length	Atom	Length
Br1—C2	1.881 (15)	C2—C1	1.37 (2)
O1—C12	1.373 (12)	C2—C3	1.407 (16)
O1—C13	1.429 (16)	C1—H1	0.9300
O2—H2	0.8200	C1—C6	1.420 (18)
O2—C5	1.337 (15)	C5—C6	1.409 (13)
N2—C9	1.34 (2)	C6—C7	1.43 (2)
N2—C8	1.354 (13)	C3—H3	0.9300
N1—C7	1.289 (15)	C7—H7	0.9300
N1—C8	1.392 (18	C18—H18	0.94 (15)
C15—H15	0.9300	C18—C17	1.38 (2)
C15—C14	1.360 (18)	C18—C19	1.386 (19)
C15—C16	1.422 (16)	C8—C12	1.416 (16)
C9—H9	0.9300	C17—H17	1.10 (14)
C9—C10	1.33 (3)	C17—C16	1.388 (18)
C4—H4	0.96 (14)	C13—H13a	0.85 (16)
C4—C5	1.42 (2)	C13—H13b	0.80 (18)
C4—C3	1.36 (2)	C13—C14	1.529 (15)
C10—H10	0.9300	C14—C19	1.396 (13)
C10—C11	1.405 (18)	C16—H16	0.98 (18)
C11—H11	0.77 (18)	C19—H19	0.9300
C11—C12	1.370 (19)		

Table. 3. Selected bond angles (°) for HL.

Atom	Angle	Atom	Angle
C13—O1—C12	116.7 (10)	C7—C6—C1	119.4 (8)
C5—O2—H2	109.5	C7—C6—C5	121.6 (11)
C8—N2—C9	117.9 (11)	C2—C3—C4	121.7 (13)
C8—N1—C7	120.9 (9)	H3—C3—C4	119.1 (7)
C14—C15—H15	120.3 (6)	H3—C3—C2	119.1 (9)
C16—C15—H15	120.3 (7)	C6—C7—N1	120.0 (9)
C16—C15—C14	119.5 (10)	H7—C7—N1	120.0 (7)
H9—C9—N2	118.3 (7)	H7—C7—C6	120.0 (5)
C10—C9—N2	123.5 (11)	C17—C18—H18	123 (10)
C10—C9—H9	118.3 (8)	N1—C8—N2	120.6 (11)
C5—C4—H4	103 (11)	C12—C8—N2	121.1 (12)
C3—C4—H4	137 (10)	C12—C8—N1	118.3 (8)
C3—C4—C5	119.7 (9)	H17—C17—C18	117 (7)
H10—C10—C9	119.8 (8)	C16—C17—C18	120.5 (9)
C11—C10—C9	120.5 (15)	C16—C17—H17	118 (8)
C11—C10—H10	119.8 (10)	C11—C12—O1	126.3 (11)
H11—C11—C10	127 (14)	C8—C12—O1	114.1 (11)
C12—C11—C10	117.4 (14)	C8—C12—C11	119.6 (10)
C12—C11—H11	112 (13)	H13a—C13—O1	99 (11)
C1—C2—Br1	121.1 (8)	H13b—C13—O1	91 (12)
C3—C2—Br1	119.4 (11)	H13b—C13—H13a	120 (15)
C3—C2—C1	119.5 (13)	C14—C13—O1	108.2 (10)
H1—C1—C2	119.7 (6)	C14—C13—H13a	112 (9)
C6—C1—C2	120.6 (9)	C14—C13—H13b	120 (10)
C6—C1—H1	119.7 (6)	C13—C14—C15	121.4 (9)
C4—C5—O2	118.3 (9)	C17—C16—C15	119.0 (12)
C6—C5—O2	122.1 (12)	H16—C16—C15	118 (7)
C6—C5—C4	119.5 (11)	H16—C16—C17	123 (7)
C5—C6—C1	118.9 (12)	C14—C19—C18	119.3 (12)

Table. 4. Intermolecular hydrogen bonds and weak intermolecular hydrogen bond geometry for HL [Å and °].

D-H...A	d(D-H)	d(H...A)	d(D...A)	<(DHA)
O2-H2...N1	0.82	1.85(4)	2.565 (13)	145 (6)
C19-H19...O1^{i}	0.93	2.78(2)	3.392 (16)	124 (1)
C19-H19...O2^{i}	0.93	2.90(1)	3.464 (14)	121 (1)

Symmetry code used: (i) -x+1,-y+1,-z+1/2

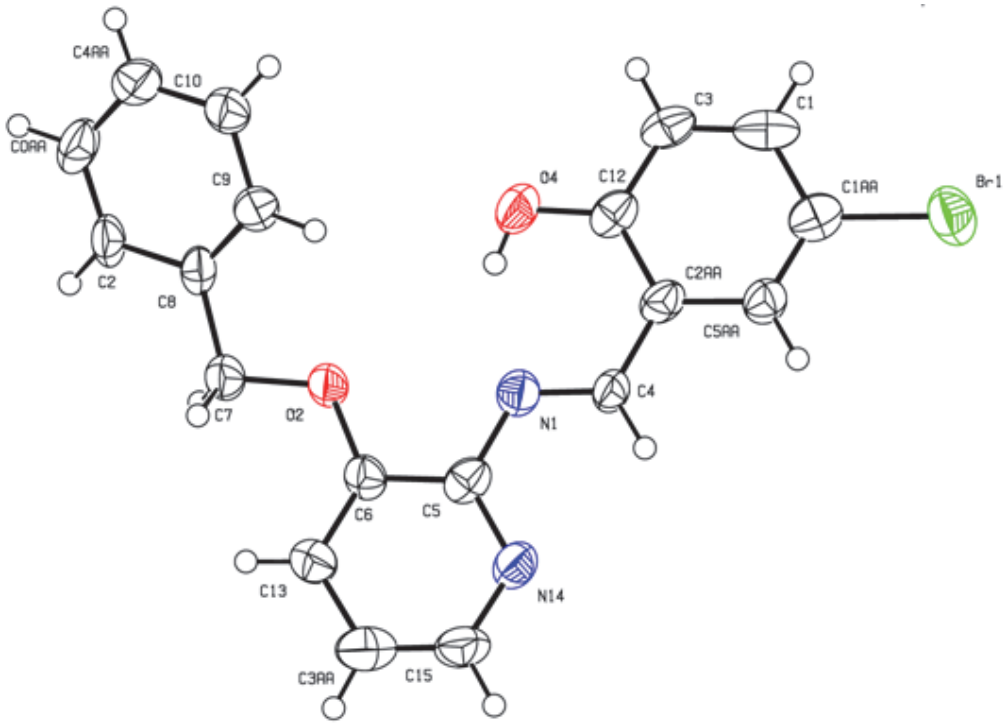

Fig. 1. ORTEP structure view of the HL.

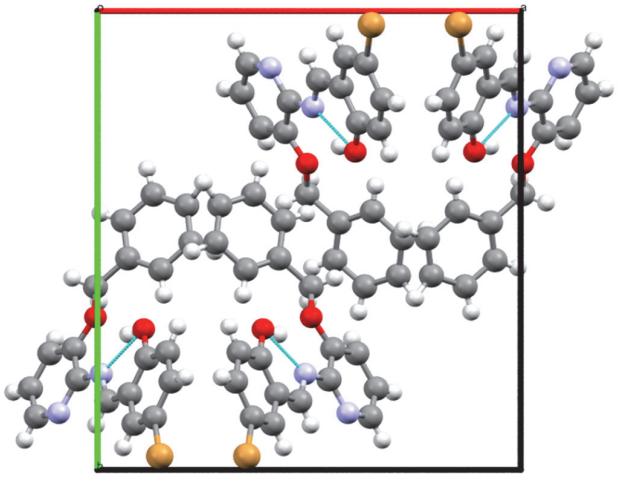

Fig. 2. Crystal packing diagram viewed along b with O2—H2--N1 intermolecular hydrogen bond is shown as a light blue dashed line

2.2. Hirshfeld-surface analysis

Hirshfeld surface analysis is an effective tool for exploring packing modes and intermolecular interactions in molecular crystals, as they provide a visual picture of intermolecular interactions and of molecular shapes in a crystalline environment. Surface features characteristic of different types of intermolecular interactions can be identified, and these features can be revealed by colour coding distances from the surface to the nearest atom exterior (d_e plots) or interior (d_i plots) to the surface. This gives a visual picture of different types of interactions present and also reflects their relative contributions from molecule to molecule.

Hirshfeld surfaces and their associated two-dimensional fingerprint plots have been used to quantify the various intermolecular interactions in the title ligand.[12,13] The two dimensional fingerprint plots from Hirshfeld surface analyses along with the electrostatic potential plots, illustrate the difference between the intermolecular interaction patterns and the relative contributions to the Hirshfeld surface (in percentage) for the major intermolecular contacts associated with the title ligand.

The intermolecular interactions of the title ligand are shown in the 2D fingerprint plots shown in **Fig. 4**. H---H (34.20%) contacts make the largest contribution to the Hirshfeld surfaces, while the N---H, O--H, H--Br and C---H interactions which make up 7.0, 8.2, 13.3 and 27.9 %of the surface. Plots also reveal the information regarding the intermolecular hydrogen bonds thus supporting for O—H…N intermolecular interactions. This intermolecular contact is highlighted by conventional mapping of d_{norm} on molecular Hirshfeld surfaces and is shown in **Fig. 3**. The red spots over the surface indicate the inter contacts involved in hydrogen bond. The dark-red spots on the d_{norm} surface arise as a result of the short interatomic contacts, i.e., weak C—H…O hydrogen bonds, while the other intermolecular interactions appear as light-red spots.

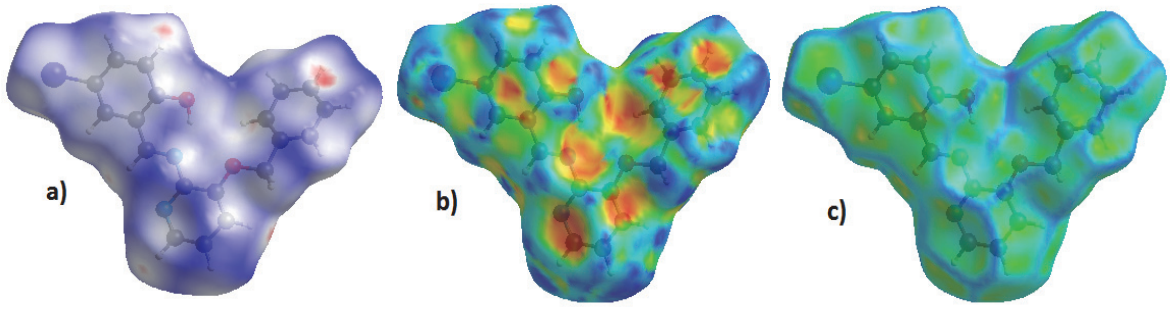

Fig. 3. Hirshfeld surface mapped with a) d_{norm} for visualizing the intermolecular interactions of the HL b) Shape index property for a compound HL c) Hirshfeld surface mapped over curvedness

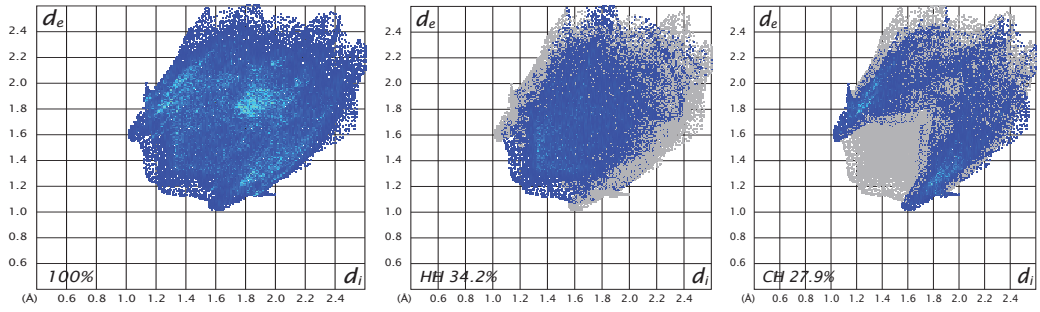

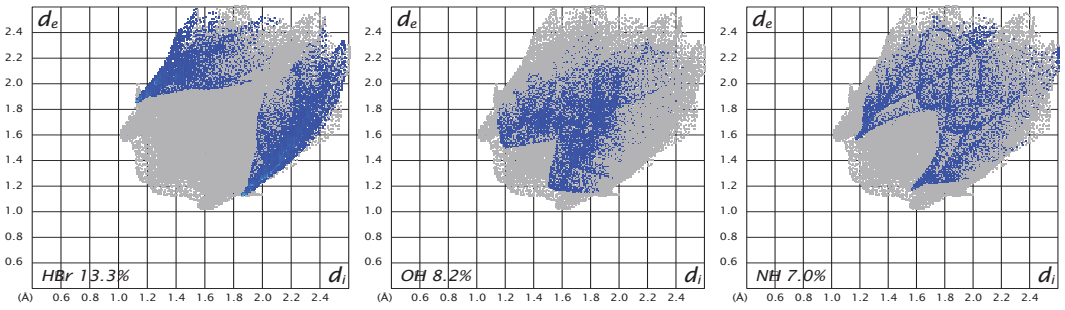

Fig. 4. d) Fingerprint plots and corresponding surface area of the title compound showing the individual contribution of each interaction. d_i is the closest internal distance from a given point on the Hirshfeld surface and d_e is the closest external contacts.

2.3. FTIR spectra

The relevant FTIR data for the ligand and its metal complexes are given in **Table 5.** The strong band is observed at 1617 cm^{-1} in the spectra of the free Schiff base ligand is a characteristic of the azomethine *ν*(C=N) stretching vibrations and it is disappeared upon coordination with metal ion.[14] The shifting of this group to lower frequency (1564-1591 cm^{-1}) in the metal complexes suggest the bonding of unsaturated nitrogen of the azomethine group of HL to the metal ions. The presence of a broad peak in the range 3500-3450 cm^{-1} indicates the presence of water molecule. The band for phenolic oxygen ν(Ph–O) occurs at 1277 cm^{-1}, whereas in complexes, this band is shifted to different frequency showing a strong band at around 1262-1274 cm^{-1} region indicates that there existed phen O-coordination and involved in coordination with metal ion. The characteristic frequency for ligand corresponding to ether C-O showing a band around 1230 cm^{-1}, which is unaltered in the spectra of complexes. It shows that the ether C-O is not involved in the coordination.[15,16] The metal-terminal oxygen ν(V=O) of the complexes C5 and C6 occurs at 974 and 969 cm^{-1} regions, respectively, which imitates the most of the oxidovanadium(IV) complexes. The new bands existed in the range 467-488 $cm^{-1}$and 515-549 cm^{-1} provides an additional proof for M-N and M-O, respectively. The appearance of νM-N and νM-O vibrations supports the proposed mode of coordination as depicted in **Fig. 5**.

Table. 5. FTIR spectral data of the Schiff base ligand [HL] and its metal complexes

Compound	ν(C=N)	ν(Ph-O)	ν(V=O)	ν(M-O)	ν(M-N)
HL	1602	1277	—	—	—
C1	1569	1274	—	475	515
C2	1577	1265	—	467	539
C3	1564	1270	—	488	527
C4	1567	1262	—	469	543
C5	1588	1273	974	472	519
C6	1591	1269	969	481	549

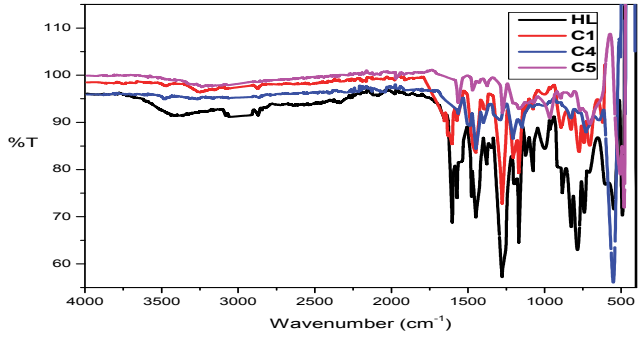

Fig. 5. IR spectra of HL and its metal complexes

2.4. Electronic spectra and magnetic moment Studies

The UV–Vis spectra of complexes in DMSO were recorded in the range of 200–800 nm as shown in **Fig. 6**. The geometry of metal complexes has been deduced from electronic spectra data of the complexes. The electronic spectra of Co(III) complexes shows a broad band at around 259-272, 304-341 and a shoulder at 574-616 nm, which may tentatively be assigned to $^4T_{1g}(F) \rightarrow {}^4T_{1g}(P)$ and $^4T_{1g}(F) \rightarrow {}^4A_{2g}(F)$, respectively, indicating an octahedral configuration around cobalt ion.[17] The electronic spectra of Ni(II) complexes are measured in DMSO exhibits bands at 254-258, 307-347 and 592-612 nm assigned to the $\pi \rightarrow \pi^*$ intraligand transition band charge transfer transition $^3A_{2g}(F) \rightarrow {}^3T_{2g}(F)$ from the metal to antibonding orbital of the ligand and $^3A_{2g}(F) \rightarrow {}^3T_{1g}(P)$ transitions, respectively, in an octahedral geometry around Ni(II) ion.[18] The observed magnetic moment values were found in the range of 3.3–3.4 BM, which is in the usual range of reported octahedral around the Ni(II) ion.[19] The electronic spectra of VO(IV) complexes show low intensity d-d bands at 257-274, 321-341 and 569-583 nm assigned to $^2b_2 \rightarrow {}^2e$, $^2b_2 \rightarrow {}^2b_1$ and $^2b_2 \rightarrow {}^2a_1$ transitions, respectively, and it is in conformity with square pyramidal geometry around VO(IV).[20] The room temperature μ_{eff} value for the vanadium complexes were found in the range 1.71-1.74 B.M. The magnetic susceptibilities of the complexes are consistent with square-pyramidal geometry around the central metal ion.[21]

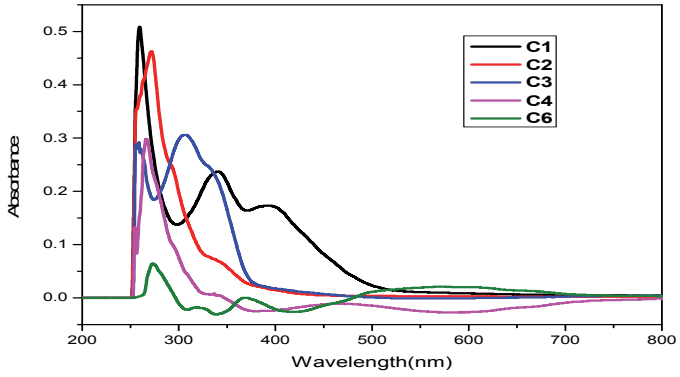

Fig. 6. The Electronic spectra of Co(III), Ni(II) and VO(IV) complexes.

2.5. Thermal analysis

Thermogravimetric analysis of representative samples has been studied as a function of temperature from room temperature to 800 °C under a nitrogen atmosphere at a heating rate of 10 °C /min. In the cobalt -complexes the first weight loss of 6.57% (calcd. 6.69%) in the 157–229 °C range indicates the loss of coordinated water and chlorine molecules. The second and third steps correspond to the complete loss of the ligand molecule in the temperature range between 230–480 and 481–567 °C with a mass loss of 27.62% (calcd.27.89) and 17.39% (calcd.17.75%), respectively. Finally the most stable CoO is formed. Thermal analysis of Ni-complexes can be divided into three stages. In the first stage, weight loss is in the range 50–130 °C having mass loss of 13.27% (calcd.13.98%) due to loss of coordinated water and chloride ion. In continuation to the first stage, gradual weight loss in the range 150-370 °C having mass loss of 35.77% (calcd. 36.05%) shows partial decomposition of the ligand moiety around the metal ion. The degradation stage is in the range of 390 -550 °C with an estimated mass loss of 33.27% (calcd. 33.77%). This mass loss corresponds to the pyrolysis of ligand molecules leaving NiO as a residue. And, one 1, 10-phenanthroline moiety were decomposed at 560–660 °C, with mass losses of 29.07% (calcd. 29.57 %) and 30.62% (calcd. 31.17 %) leaving behind the corresponding metal oxide respectively. The vanadium- complexes decomposes in two stages. The first stage degradation starts at 190-244 °C with an estimated weight loss of 35.07% (calcd.35.68%) due to loss of phenanthroline. Further decomposition occurs in the temperature range of 250- 460 °C having mass loss of 42.57% (calcd. 42.79) indicates the loss of coordinated ligand. Further

decomposition occurs in the temperature range of 550-670 °C corresponds to the final residue estimated as free vanadium oxide[22] and is shown in **Fig. 7**. On the basis of above facts, the proposed structure of metal complexes are presented in **Fig. 8**.

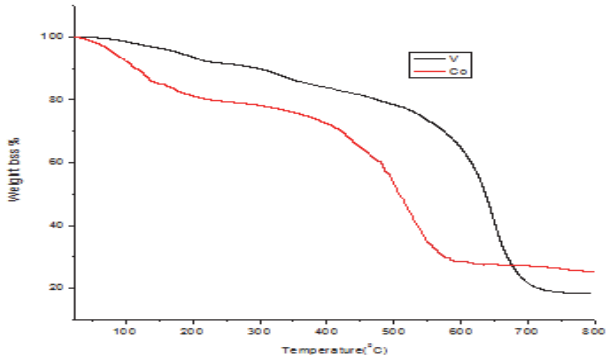

Fig. 7. Thermograms of cobalt and vanadium complexes

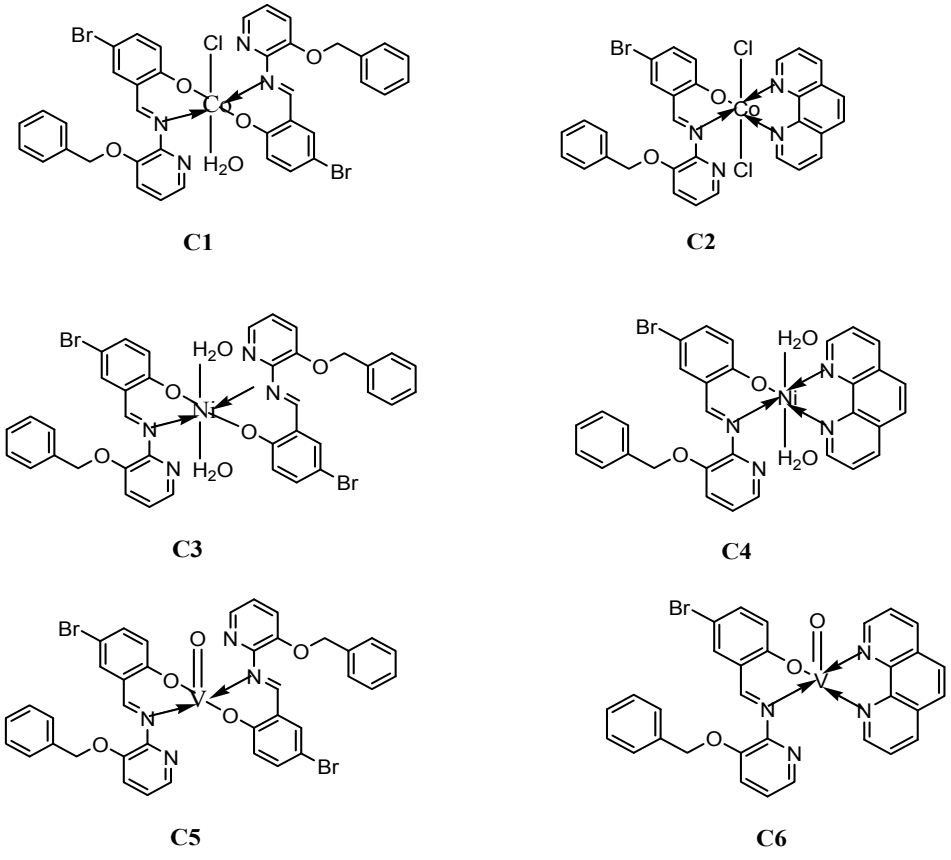

Fig. 8. Proposed structures of the prepared metal complexes

2.6. Biological activity

2.6.1. Antimicrobial activity

The synthesized compounds of cobalt, nickel and vanadium complexes were screened for antibacterial activities against Gram positive bacteria *Bacillus subtilis* (ATCC 21332), *Staphylococcus*

aureus (ATCC 25923) and Gram negative bacteria *Salmonella typhi* (19430), *Escherichia coli* (ATCC 25922) and antifungal activities against *Aspergillus niger* (MTCC 1881), *Aspergillus lavus* (MTCC 873), *Candida albicans* (MTCC 227) and *Alternaia Solani* (MTCC 4634) by well diffusion method.[23] Chloramphenicol and fluconazole were used as standards drugs for the comparison of the results. The minimum inhibitory concentration (MIC) profile of the entire compounds against bacteria and fungi are summarized in **Tables 6** and **Table 7**. Four bacterial stains were incubated for 24 h at 37 °C, and fungal stains were incubated for 48 h at 37 °C along with standard antibacterial drug under similar conditions for comparison. The fungi were subcultured in potato dextrose agar medium, and the standard antifungal drug, fluconazole was used for control. Stock solution (10^{-3} M) was prepared by dissolving the compounds in DMSO. Development of any turbidity illustrated that the compound was not able to inhibit the growth, while no turbidity indicated the inhibition of microorganism by the sample. All the studies were performed in triplicates and the average zone of inhibition was taken as the final reading.

Table. 6. Antimicrobial results of the Schiff base ligand and its metal complexes.

Compound	Zone of inhibition (in mm)							
	Antibacterial				Antifungal			
	Gram-positive bacteria		Gram-negative bacteria					
	B. subtilis	*S. aureus*	*S.typhi*	*E.coli*	*A.niger*	*A. flavus*	*C.albicans*	*A.solani*
HL	15	13	17	11	10	13	11	9
C1	21	19	20	23	18	16	15	13
C2	29	27	24	28	19	14	13	15
C3	34	28	31	29	23	22	27	24
C4	27	22	28	31	16	20	17	19
C5	32	30	31	33	22	20	23	24
C6	28	27	30	29	20	15	17	18
Chloramphenicol	38	33	26	35	--	--	--	--
Fluconazole	--	--	--	--	27	24	29	26

The outcome in the above studies shows that the activity of the complexes is higher than that of the corresponding ligand and this activity enhanced on coordination with metal ions. This enhancement in the activity may be rationalized on the basis that ligands mainly posses C=N bond. The enhanced antimicrobial activity of the complex compared with its ligand can be explained using chelation theory.[24] The increase in antimicrobial activity may be considered in light of Searl's concept and Tweedy's chelation theory.[25, 26, 27]

Table. 7. MIC [μg/ml] values for antimicrobial activity of Schiff base ligand and its corresponding metal complexes

Compound	Bacteria				Fungi			
	Gram-positive bacteria		Gram-negative bacteria					
	B. subtilis	*S. aureus*	*S.typhi*	*E.coli*	*A.niger*	*A. flavus*	*C.albicans*	*A.solani*
HL	>100	>100	>100	>100	>100	>100	>100	>100
C1	71	66	69	73	68	72	77	63
C2	74	72	70	71	59	68	73	70
C3	83	78	81	72	77	82	74	80
C4	79	77	75	74	72	65	77	79
C5	74	76	81	83	80	78	85	75
C6	78	73	67	65	71	69	73	77
Chloramphenicol	37	37	37	37	--	--	--	--
Fluconazole	--	--	--	--	37	37	37	37

3. Conclusion

In the present work, Co(III), Ni(II) and VO(IV) complexes were prepared from novel Schiff base and are characterized using various spectral techniques. The IR spectral data demonstrate that the ligand acts as a bidentate, coordinating through azomethine nitrogen and carbonyl oxygen atoms. Thermal data provided the number of coordinated and lattice water molecules in the complexes. Magnetic and electronic spectral studies revealed octahedral geometry for Co(III) and Ni(II) complexes and square-

pyramidal for VO(IV) complexes. The crystal structure of ligand HL has also been determined by X-ray diffraction studies. The ligand and its Co(III), Ni(II) and VO(IV)complexes were tested for antimicrobial activity against some pathogen. Antimicrobial study reveals that, metal complexes have more biological activity than free ligand.

Acknowledgements

The author Disha Sharma is thankful to the University of Mysore, Mysuru for laboratory facilitates. Also, wish to thank Sagar BK for X-ray diffraction and Hirshfeld surface analysis. I also like to acknowledge Institute Of Excellence, University of Mysore, Mysuru for providing Instrumentation Facility.

4. Experimental

4.1. Materials and methods

All the reagents, starting materials as well as solvents were purchased commercially and used without any further purification. 1, 10-phenanthroline monohydrate and $CoCl_2.6H_2O$, $NiCl_2.6H_2O$ and $VOSO_4.2H_2O$ obtained from Merck Specialties Private Limited, Mumbai were used. Melting point was determined in open capillary tube using Precision Digital Melting Point Apparatus and is uncorrected. Elemental analysis was performed on Perkin Elmer 240 CHN-analyzer. ^1H and ^{13}C NMR spectra were obtained on Varian-400 MHz spectrometer using TMS (Tetra methyl silane) as an internal reference (Chemical shifts in δ, ppm) in $CDCl_3$ solvent. Electrospray ionization (ESI) mass spectra were recorded using a 2010EV LCMS Shimadzu spectrometer. Infrared spectra were measured using Perkin Elmer Spectrum Version 10.03.09.in the range of 4000-400 cm^{-1}. The magnetic susceptibility of the solid complexes was determined by Gouy method at room temperature (27±3°C) using $Hg[Co(SCN)_4]$ as the standard. Molar conductance in $\sim 10^{-3}$ M DMSO solution was recorded using an Elico Cm-180 conductometer. Electronic spectra of the complexes in the UV-visible region (200-800nm) were measured using an ELICO SL 117 double beam spectrophotometer with quartz cells. TG and DTA measurements for the complexes were recorded in nitrogen atmosphere on TGA Q50 instrument keeping the final temperature at 800 °C with the heating rate of 10 °C/min.

4.2. Synthesis of ligand and its complexes

4.2.1. Synthesis of (E)-2-((3-(benzyloxypyridinylimino) methyl)-4-bromophenol (HL)

A new Schiff base was prepared (as shown in scheme, **Fig. 9**) by the condensation of equimolar amounts of 2-amino-3-benzyloxypyridine (0.002 mol) and 5-bromo salicylaldehyde (0.002 mol) were taken in round bottom flask containing minimum quantity of ethanol. The reaction mixture was refluxed with a catalytic amount of glacial acetic acid (1-2 drops) for about 7-8 h on a water bath at a temperature of 70-80 °C. The progress of the reaction was monitored by TLC. On completion of the reaction, the product was separated by filtration, washed and dried over anhydrous $CaCl_2$ in desiccator and recrystallized from ethanol. Mass spectrum, ^1H NMR, ^{13}C NMR and FT IR spectrum of HL are depicted in **Figs. (10-13)**. The developed single crystal was used to elucidate the structure of HL by single crystal X-ray diffractometer.

Ligand (HL): Orange, Yield 87%, melting point 128-130 °C. CHN found (calc.) for $C_{19}H_{15}BrN_2O_2$: C: 59.55(60.07), H: 3.95(3.14), N: 7.31(6.96); MS (m/z): 383[M^+]; Found: 385[M+2]; FTIR υ (cm^{-1}); ν (OH) 3406, ν (C=N) 1617; ^1H NMR (400 MHz, $CDCl_3$); 9.36(s, HC=N), 14.22(s, Ph-OH), 6.91-8.0(m, Ar–H), 5.22(-CH_2-O); ^{13}C NMR (400 MHz, $CDCl_3$); 161.816, 161.545, 148.771, 147.071, 140.203, 136.219, 135.976, 134.906, 128.706, 128.145, 126.953, 123.720, 121.459, 120.700, 119.623, 110.114, 77.293, 76.974, 76.655. UV-Vis (DMSO): λmax=376 nm.

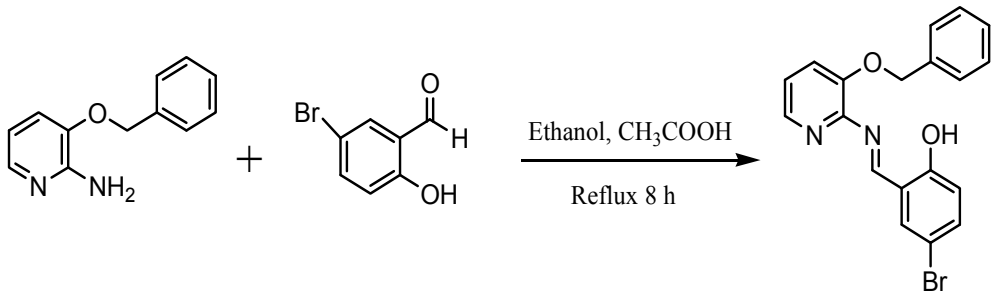

HL

Fig. 9. Schematic representation of synthesis of Schiff base ligand

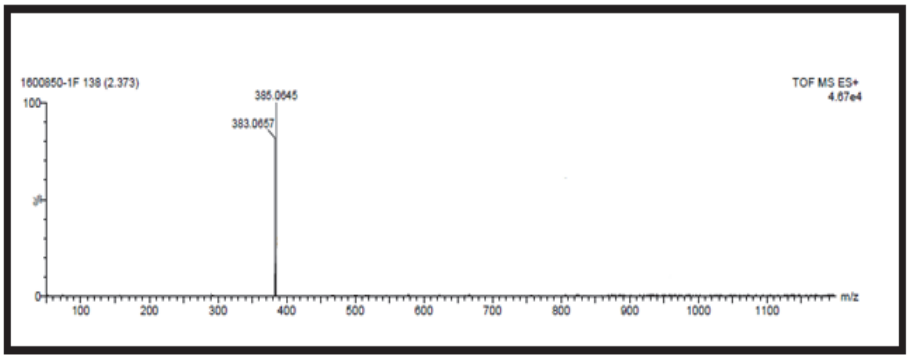

Fig. 10. MS spectrum of HL

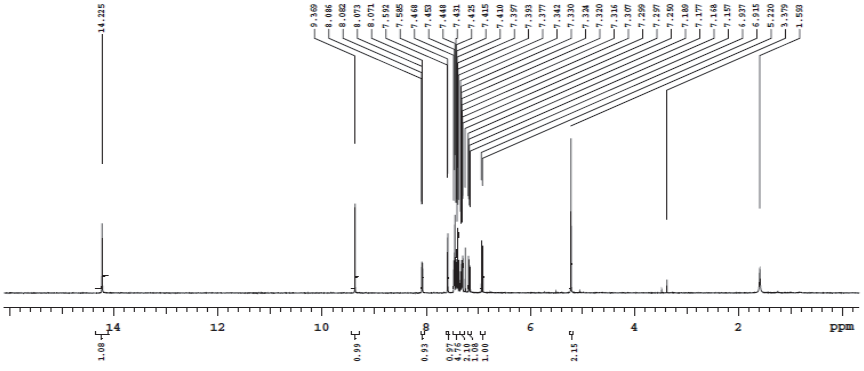

Fig. 11. [1]H-NMR of HL

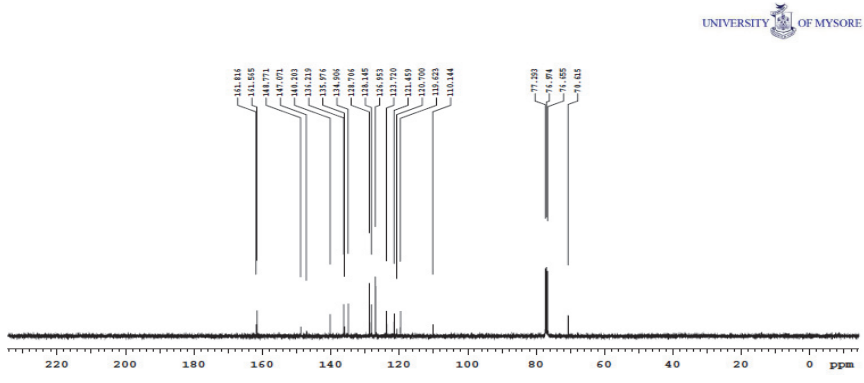

Fig. 12. [13]C-NMR of HL

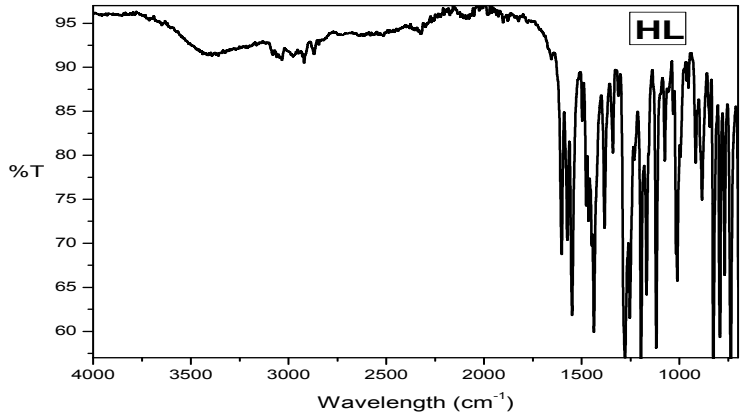

Fig. 13. FT IR spectrum of HL

4.2.2. Preparation of complexes C1, C3 and C5 in the ratio of 1:2

The ethanolic solutions of corresponding metal salts (1 mmol) were added slowly to a hot ethanolic solution of Schiff base ligand HL (2 mmol). The reaction mixture was refluxed for 6 h at 70 °C on water bath. The precipitate obtained was filtered, washed with ethanol and dried in desiccators using calcium chloride.

4.2.3. Preparation of complexes C2, C4 and C6 in the ratio of 1:1:1

The complexes were prepared by mixing equimolar ethanolic solutions of metal salts (1 mmol) and ligand (1 mmol) with stirring for 30 minutes. A solution of 1, 10-phenanthroline monohydrate (Phen) (1 mmol) dissolved in 10 ml ethanol was added to the reaction mixture. It was continued to reflux for 6 h on water bath. Then evaporated the solvent and the resulting complexes were used for further analysis. The development of single crystal of the metal complexes is unsuccessful.

4.3. Crystal structure determination by X-ray crystallography

Single crystal X-ray diffraction data of the Schiff base ligand HL was collected on a Bruker, Microstar Proteum 8 diffractometer, with Cu-Kα radiation (λ=1.54178 °A) at 296 K. The structure was solved by direct methods using SHELXS-86 and refined by full-matrix technique using SHELXL-2014.[28,29] All the non-hydrogen atoms were refined anisotropically. The summary of pertinent crystal data along with further details of structure determination and refinement are given in **Table 8**. The ORTEP, planes and packing diagrams were generated using the Mercury 3.8 software.

Table. 8. Crystal data and structure refinement parameters of the HL.

Identification code	HL	
CCDC deposition number	1585783	
Empirical formula	$C_{19}H_{15}BrN_2O_2$	
Formula weight	383.2	
Temperature	296 K	
Wavelength	1.54178 Å	
Crystal system	orthorhombic	
Space group	$Pca2_1$	
Unit cell dimensions	a = 14.240(3) Å	α= 90°
	b = 16.090(3) Å	β= 90°
	c = 7.2170(7) Å	γ = 90°
Volume	1653.5(5) $Å^3$	
Z	4	
Density (calculated)	1.539 Mg/m^3	
Absorption coefficient	3.50 mm^{-1}	
F(000)	775.0352	
Crystal size (in mm)	0.31 x 0.29 x 0.28	
Theta range for data collection	5.5to 64.0	

Data collection	
Index ranges	$-16 \leq h \leq 15$, $-16 \leq k \leq 18$, $-7 \leq l \leq 8$
Reflections collected	6340
Independent reflections	2173
Criterion for observed reflections	$I > 2\sigma(I)$
Refinement	
Refinement method	Full-matrix least-squares on F^2
Data / restraints /constraints / parameters	2173 / 01/ 23/ 242
Goodness-of-fit on F^2	1.20
Final R indexes [I>=2σ (I)]	$R_1 = 0.138$, $wR_2 = 0.309$
R indices (all data)	$R_1 = 0.2051$, $wR_2 = 0.3094$
H-atom parameters treatment	mixture of independent and constrained refinement
$(\Delta/\sigma)_{max}$	0.867
Largest diff. peak and hole	$\Delta\rho_{max} = 2.93$ Å^{-3}, $\Delta\rho_{min} = -0.53$ e Å^{-3}

4.4. In-vitro Antimicrobial Screening

In vitro antimicrobial screening effects of the ligand and its metal complexes were tested for their antibacterial and antifungal activities using disc diffusion method. Chloramphenicol and fluconazole are the standards for antibacterial and antifungal activities, respectively. All the experiments were performed in triplicate and the average zone of inhibition was recorded. To get the required test solutions, the compounds were dissolved in DMSO. The compounds which show significant activities were selected to determine the minimum inhibitory concentration (MIC) using well diffusion technique.

References

1. Isloor A. M., Kalluraya B., and Shetty P. (**2009**) Regioselective reaction: synthesis, characterization and pharmacological studies of some new Mannich bases derived from 1,2,4-triazoles. *Eur. J. Med. Chem.* 44 (9) 3784–7.
2. Mohareb R. M., El-Sayed N. N. E. and Abdelaziz M. A. (**2012**) Uses of Cyanoacetylhydrazine in Heterocyclic Synthesis: Novel Synthesis of Pyrazole Derivatives with Anti-tumor Activities. *Molecules* 17 (7) 8449–63.
3. Ziegler J., Schuerle T., Pasierb L., Kelly C., Elamin A., Cole K. A., and Wright D. W. (**2000**) The Propionate of Heme Binds N_4O_2 Schiff Base Antimalarial Drug Complexes. *Inorg. Chem.* 39 (16) 3731–3733.
4. Annapoorani S., and Krishnan C. N. (**2013**) Synthesis And Spectroscopic Studies Of Trinuclear N4 Schiff Base Complexess, *J. Chem. Tech. Res*. 5 (1) 180-185.
5. Shoaib K., Rehman W., Mohammad B. and Ali S. (**2013**) Synthesis, Characterization and Biological Applications of Transition Metal Complexes of [no] Donor Schiff Bases. *J. Proteomics Bioinform.* 6 (7) 153–7.
6. Chang H. Q., Jia L., Xu J., Zhu T. F., Xu Z. Q., and Chen R. H. (**2016**) Syntheses, crystal structures, anticancer activities of three reduce Schiff base ligand based transition metal complexes. J. Mol. Struct. 1106, 366–72.
7. Khamamkar A. and Pallapothula V. R. (**2014**) Synthesis and charecterisation of complexes derived from succinyl dihydrazide and 3-acetyl-6- methyl-2H-pyran-2, 4(3H)-dione. *Acta Biomed. Sci.* 1 (4) 179-184.
8. Temel H., and Sekerci M., (**2001**) Novel complexes of manganese(iii), cobalt(ii), copper(II), and zinc(II) with Schiff base derived from 1,2-bis(p-amino-phenoxy)ethane and salicylaldehyde. S*ynth. React. Inorg. Met. Org. Chem.* 31 (5) 849-57.
9. Watanabe K., Ohta T., and Shirasu Y. (**1989**) Enhancement and inhibition of mutation by o-vanillin in Escherichia coli. *Mutat. Res*.218 (2) 105-9.
10. Pelgrift R. Y., and Friedman A. J. (**2013**) Nanotechnology as a therapeutic tool to combat microbial resistance. *Adv. Drug Deliv. Rev.* 65 (13–14) 21803–1815.
11. Boyd D. B. (**1983**) Substituent effects in cephalosporins as assessed by molecular orbital calculations, nuclear magnetic resonance, and kinetics. *J. Med. Chem.* 26 (7) 1010-1013.

12. Spackman M. A., and McKinnon J. J. (**2002**) Fingerprinting intermolecular interactions in molecular crystals. *CrystEng Comm.* 4 (66) 378–392.
13. Soman R., Sujatha S., Sushmita De., Rojisha V.C., Parameswaran P., Varghese B., and Arunkumar C. (**2014**) Intermolecular Interactions in Fluorinated Tetraarylporphyrins: An Experimental and Theoretical Study. *Eur. J. Inorg. Chem.* 2014 (16) 2653–2662.
14. Kumar L. S., Prasad K. S., and Revanasiddappa H. D. (**2013**) SODs, DNA binding and cleavage studies of new Mn(III) complexes with 2-((3-(benzyloxy)pyridin-2-ylimino)methyl)phenol. *Spectrochim Acta A Mol Biomol Spectrosc.* 107, 203–212.
15. Ma J-X., Li Q-L., Li P-P., Zhao J-X., and Zhao L. (**2018**) Crystal structure of bis{5-methoxy-2-((*E*)-((4-((*E*)-1-(methoxyimino)ethyl)phenyl)imino)methyl)phenolato-κ ^{2}*N,O*}nickel(II), $C_{34}H_{34}N_4NiO_6$. *Z. Kristallogr. - New Cryst. Struct.* 233 (5) 767-769.
16. Hong Y., Liu W., and Gou G. (**2018**) Crystal structure of [4-chloro-2-(((2-((3-ethoxy-2-oxidobenzylidene)amino)phenyl)imino)(phenyl)methyl)phenolato-κ^4*N*,*N*′,*O*,*O*′}nickel(II) - ethyl acetate (1/1), $C_{32}H_{29}ClN_2NiO_5$. *Z. Kristallogr. - New Cryst. Struct.* 233 (6) 989-991.
17. Neelakantan M. A., Rusalraj F., Dharmaraja J., Johnsonraja S., Jeyakumar T., and Pillai M.S. (**2008**) Spectral characterization, cyclic voltammetry, morphology, biological activities and DNA cleaving studies of amino acid Schiff base metal(II) complexes. *Spectrochim. Acta Part A* 71(4) 1599-1609.
18. Gull P., AL-Thabaiti S.A., and Hashmi A.A. (**2014**) Design, Characterization and antimicrobial activity of Cu(II), Co(II) and Zn(II) complexes with Schiff base from 1,2-diphenylethane-1,2-dione and N-(1-Naphthyl) ethylenediamine. *Int. J. Multidiscip. Curr. Res.* 2 (6) 1142-1147.
19. Kumar S., Deepak V., Kumari M., and Dutta P.K. (**2015**) Antibacterial activity of diisocyanate-modified chitosan for biomedical applications. *Int. J. Bio. Macro*. 84, 349-353.
20. Raman N., Ravichandran S., and Thangaraja C. (**2004**) Copper(II), cobalt(II), nickel(II) and zinc(II) complexes of Schiff base derived from benzil-2,4-dinitrophenylhydrazone with aniline. *J. Chem. Sci*.116 (4) 215-219.
21. Pranita U.G., Mandlik P.R., and Aswar A.S. (**2015**) Synthesis and characterization of Cr(III), Mn(III), Fe(III), VO(IV), Zr(IV) and UO2 (VI) complexes of schiff base derived from isonicotinoylhydrazine. *Indian J. Pharm. Sci.* 77 (4) 376-381.
22. Prasad K. S., Kumar L. S., Shekar S. C., Prasad M., and Revanasiddappa H. D. (**2011**) Oxovanadium Complexes with Bidentate N, O Ligands: Synthesis, Characterization, DNA Binding, Nuclease Activity and Antimicrobial Studies. *Chem. Sci. J.* 2 (1) 1-10.
23. Belaid S., Landreau A., Djebbar S., Benali-Baitich O., Bouet G., and Bouchara J. P. (**2008**) Synthesis, characterization and antifungal activity of a series of manganese(II) and copper(II) complexes with ligands derived from reduced *N*,*N*′-*O*-phenylenebis(salicylideneimine). *J. Inorg.Biochem.* 102 (1) 63–69.
24. El-Sherif A. A., Shoukry M. M., and Abd-Elgawad M. M. A. (**2012**) Synthesis, characterization, biological activity and equilibrium studies of metal(II) ion complexes with tridentate hydrazone ligand derived from hydralazine. *Spectrochim. Acta A Mol. Biomol. Spectrosc.* 98, 307-321
25. Dharamaraj N., Viswanathamurthi P., and Natarajan K. (**2001**) Ruthenium(II) complexes containing bidentate Schiff bases and their antifungal activity. *Tran. Met. Chem.* 26 (1-2) 105–109.
26. Tweedy B.G. (**1964**) Plant extracts with metal ions as potential antimicrobial agents. *Phytopathology* 55, 910-914.
27. Takjoo R., Akbari A., Ebrahimipour S.Y., Kubicki M., Mohamadi M., and Mollania N. (**2017**) Synthesis, spectral characterization, DFT calculations, antimicrobial activity and molecular docking of 4-bromo-2-((2-hydroxy-5-methylphenylimino)methyl)phenol and its V(V) complex. *Inorg. Chim. Acta* 455 (1) 173–182.
28. Sheldrick G. M. (**2008**) A short history of SHELX. *Acta cryst. A* 64. 112-122.
29. Sheldrick G. M. (**2015**) Crystal structure refinement with *SHELXL. Acta cryst. C* 71 3-8.